



**INTELLECTUAL
PROPERTY INDIA**

PATENTS | DESIGNS | TRADE MARKS
GEOGRAPHICAL INDICATIONS



सत्यमेव जयते

भारत सरकार
GOVERNMENT OF INDIA

पेटेंट कार्यालय
THE PATENT OFFICE

पेटेंट प्रमाणपत्र
PATENT CERTIFICATE
(Rule 74 Of The Patents Rules)

क्रमांक : 044118829
SL No :



पेटेंट सं. / Patent No. : 335882
आवेदन सं. / Application No. : 3951/CHE/2015
फाइल करने की तारीख / Date of Filing : 31/07/2015
पेटेंटी / Patentee : INDIAN INSTITUTE OF TECHNOLOGY MADRAS (IIT Madras)

प्रमाणित किया जाता है कि पेटेंटी को उपरोक्त आवेदन में यथाप्रकटित CELLULOSE DERIVED GRAPHENIC FIBERS FOR CAPACITIVE DESALINATION OF BRACKISH WATER AND PREPARATION METHOD OF THE ELECTRODE THEREOF नामक आविष्कार के लिए, पेटेंट अधिनियम, १९७० के उपबंधों के अनुसार आज तारीख 31st day of July 2015 से बीस वर्ष की अवधि के लिए पेटेंट अनुदत्त किया गया है।

It is hereby certified that a patent has been granted to the patentee for an invention entitled CELLULOSE DERIVED GRAPHENIC FIBERS FOR CAPACITIVE DESALINATION OF BRACKISH WATER AND PREPARATION METHOD OF THE ELECTRODE THEREOF as disclosed in the above mentioned application for the term of 20 years from the 31st day of July 2015 in accordance with the provisions of the Patents Act, 1970.



अनुदान की तारीख : 23/04/2020
Date of Grant :

Okrajt
पेटेंट नियंत्रक
Controller of Patent

टिप्पणी - इस पेटेंट के नवीकरण के लिए फीस, यदि इसे बनाए रखा जाना है, 31st day of July 2017 को और उसके पश्चात प्रत्येक वर्ष में उसी दिन देय होगी।

Note. - The fees for renewal of this patent, if it is to be maintained will fall / has fallen due on 31st day of July 2017 and on the same day in every year thereafter.

31 JUL 2015

ORIGINAL

3951 /CHE/ 20.15

FORM 2
THE PATENTS ACT, 1970
(39 OF 1970)
&
The Patents Rules, 2003
COMPLETE SPECIFICATION
(Refer section 10 and rule 13)

TITLE OF THE INVENTION:

CELLULOSE DERIVED GRAPHENIC FIBERS FOR CAPACITIVE DESALINATION OF BRACKISH WATER AND PREPARATION METHOD OF THE ELECTRODE THEREOF

2. APPLICANT:

(A) NAME: **INDIAN INSTITUTE OF TECHNOLOGY MADRAS**

(B) NATIONALITY: Indian

(C) ADDRESS: **INDIAN INSTITUTE OF TECHNOLOGY MADRAS**

IIT P.O

Chennai - 600 036

3. Preamble to the Description

COMPLETE SPECIFICATION

The following specification describes the invention

COMPLETE SPECIFICATION

TITLE OF THE INVENTION

5

CELLULOSE DERIVED GRAPHENIC FIBERS FOR CAPACITIVE DESALINATION OF BRACKISH WATER AND PREPARATION METHOD OF THE ELECTRODE THEREOF

10 FIELD OF THE INVENTION

The present invention relates to a cellulose derived graphenic fiber electrode for capacitive desalination of brackish water and preparation method of the same.

15 BACKGROUND OF THE INVENTION

Shortage of clean water is the most exigent problem faced by several communities in the developing world. Access to safe and potable water is threatened by population growth, climate change and contamination of existing fresh water sources. [*Nature Clim. Change* **2014,4**, 318-320; *PNAS***2014**, *111*, 3245-3250; *Nature* **2008,452**, 301-310]. The need for clean water for domestic, agricultural and industrial processes has resulted in intense search for alternate sources of water supply, such as brackish ground water and sea water [*Nature Clim. Change* **2014,4**, 318-320; *Nature* **2008,452**, 301-310]. Reverse osmosis (RO), ultra-filtration (UF) and distillation processes are the most widely used treatment technologies for water today [*Science* **2011**,*333*, 712-717]. However, rising proportion of concentrates being generated worldwide excessive energy requirement and need for skilled personnel to maintain such facilities are limiting their large scaled employment in resource-limited settings [*ACS Appl. Mater. Interfaces***2012,4**, 1194-1199].

Capacitive deionization (CDI) is increasingly being considered as a viable solution for water desalination that is more energy efficient than the above mentioned processes. This technology fundamentally involves adsorption of oppositely charged ions from the electrical double layer region over an electrode upon application of a potential leading to desalination. Subsequent desorption of the adsorbed ions when the potential is reversed leads to regeneration of the electrodes [*ACS Appl. Mater. Interfaces***2012,4**, 1194-1199; *Prog. Mater. Sci.***2013,58**,

1388-1442; *Energy Environ. Sci.* **2012**,*5*, 9511-9519; *Environ. Sci. Technol.* **2014**,*48*, 2008-2015; *Environ. Sci. Technol.* **2011**,*45*, 10243-10249]. Although CDI is associated with high theoretical efficiency, cost effectiveness and point-of-use (POU) utility, its practical applications for desalination are yet to be realized fully [*Prog. Mater Sci.* **2013**,*58*, 1388-1442; *Energy Environ. Sci.* **2012**,*5*, 9511-9519; *Environ. Sci. Technol.* **2014**,*48*, 2008-2015; *Environ. Sci. Technol.* **2011**,*45*, 10243-10249]. The existing mainstream CDI materials with their inherent limitations in stability and resistance to biofouling confine such electrodes for larger scale operations. Various methods are used to solve these issues and commercial products are available; although capital costs are higher than RO. An ideal CDI material should exhibit the following characteristics: high specific surface area, high conductivity, fast adsorption/desorption rates, electrochemical stability, resistance to biofilm formation, and easy processability [*Prog. Mater Sci.* **2013**,*58*, 1388-1442; *Desalination* **2008**, *228*, 10-29; *J. Phys. Chem Lett.* **2009**, *1*, 205-210].

The salt removal efficiency of various forms of carbon used as an electrode for CDI is generally reported in terms of salt (NaCl) adsorbed per gram of carbon. Li *et al.* and Kim *et al.* reported the capacity to be 0.275 and 3.7 mg/g, respectively for activated carbon [*Carbon* **2009**, *47*, 775-781; *Sep. Purif. Technol.* **2010**, *71*, 70-75]. In addition, multi-walled carbon nanotubes [*Mater. Lett.* **2005**, *59*, 1989-1992], single-walled carbon nanotubes [*J. Electroanal. Chem.* **2011**, *653*, 40-44], graphene-like nanoflakes [*Environ. Sci. Technol.* **2010**, *44*, 8692-8697], graphene [*J. Mater. Chem.* **2009**, *19*, 6773-6779], graphene-carbon nanotubes [*J. Mater. Chem.* **2012**, *22*, 14696-14704], carbon nanofiber webs [*Electrochim. Acta* **2012**, *69*, 65-70], reduced graphene oxide-activated carbon [*J. Mater. Chem.* **2012**, *22*, 15556-15561], Ti-O activated carbon cloth [*Water Res.* **2003**, *37*, 1527-1534] and MnO₂ activated carbon [*Desalination* **2011**, *276*, 199-206] have shown adsorption capacities of 1.7, 0.75, 1.3, 1.8, 1.4, 4.6, 2.9, 4.3 and 1.0 mg/g, respectively. These systems are excellent in terms of electrical conductivity and pore-distribution, but are found lacking in their symmetric adsorption and desorption of counter ions, electrochemical stability and resistance to biofouling. Additionally, they suffer from a relatively complicated manufacturing process and high production cost [*Prog. Mater Sci.* **2013**, *58*, 1388-1442]. In comparison, mesoporous carbon is inexpensive, highly porous material with a varying pore size than activated carbon (< 2nm). This property can help overcome the limited ion accessibility and slow diffusion associated with activated carbon [*Environ. Sci. Technol.* **2011**,

45, 10243-10249; *J. Mater. Chem.* **2010**, *20*, 4602-4608; *J. Mater. Chem.* **2012**, *22*, 6603-6612; *Energy Environ. Sci.* **2013**, *6*, 3700-3712; *The J. Phys. Chem. C* **2011**, *115*, 17068-17076].

However, the obtained adsorption efficiency is less due to the high inner electrode resistance of the mesoporous carbon [*J. Mater. Chem.* **2010**, *20*, 4602-4608; *Energy Environ. Sci.* **2013**, *6*, 3700-3712; *Sep. Purif. Technol.* **2013**, *103*, 216-221]. Incorporation of conducting polymers, metal oxides, graphene and carbon nanotubes into mesoporous carbon is an effective approach for solving this issue [*J. Mater. Chem.* **2012**, *22*, 6603-6612; *Water Res.* **2010**, *44*, 990-996; *Adv.* **2014**, *4*, 64634-64642; *Desalination* **2014**, *342*, 70-74; *J. Mater. Chem. A* **2013**, *1*, 11778-11789; *J. Mater. Chem. A* **2014**, *2*, 4739-4750; *J. Mater. Chem. A* **2013**, *1*, 6335-6341]. Though these agents locally impart a pseudo capacitance on the surface, they do not contribute much to the adsorption efficiency. Recently, incorporating graphene into a mesoporous carbon increased its conductivity, as a result, it leads to higher adsorption of salt from brackish water compared to carbon electrode alone [*Carbon* **2009**, *47*, 775-781; *J. Mater. Chem.* **2012**, *22*, 15556-15561].

With an objective to develop a cost effective and superior CDI electrode material with high surface area, low electrical resistance and electrochemical durability, the present invention synthesizes a layer-by-layer stacked graphite reinforced-cellulose (GrC) derived 3D mesoporous fibrous carbon electrode. The material exhibits the above mentioned characteristics along with superior adsorption capability and resistance to bacterial biofilm formation, while being cost effective. The CDI performance of this hybrid electrode was evaluated and the effect of biofouling was examined via a temporal study employing a biofilm-forming organism, *Pseudomonas putida*. These characteristics make the present invention, graphite-reinforced cellulose derived carbon fiber material as a promising candidate for POU water treatment in resource-limited settings.

25 SUMMARY OF THE INVENTION

The present invention describes a graphite reinforced-cellulose (GrC) derived 3D mesoporous fibrous carbon electrode for capacitive deionization.

Some embodiments of the present invention relate to a capacitive deionization apparatus having improved desalination efficiency.

Another aspect of the invention relates to synthesise of reinforced-cellulose (GrC) derived carbon electrode by a layer-by-layer method.

Some embodiment of the present invention relate to electro-adsorption of NaCl on the graphite reinforced-cellulose (GrC) electrode which reached equilibrium quickly (within 90 min) and the adsorbed salts were released swiftly (in 40 min) back into the solution, during reversal of the terminal.

Another aspect of the invention relates to GrC electrode with highest electro-adsorption capacity of 13.1 mg/g at a cell potential of 1.2 V, with excellent recyclability and complete regeneration.

Some embodiment of the present invention relate to electrode having high tendency for removal of specific anions, such as fluoride, nitrate, chloride and sulphate from water in the following order: $Cl^- > NO_3^- > F^- > SO_4^{2-}$.

Other aspect of the invention relate to surface morphology of graphenic carbon fiber electrode which provides resistance against bacterial adhesion and proliferation but not limited to biofouling and biofilm formation by *Pseudomonas putida*.

According to the embodiments of the present invention, the graphite reinforced-cellulose (GrC) derived carbon fiber electrode provides uniform conductivity throughout the electrode with fast electro-adsorption, rapid desorption and extended reuse making the electrode affordable for capacitive desalination of brackish water in resource limited settings.

BRIEF DESCRIPTION OF THE DRAWINGS:

Figure 1 provides a schematic representation of the procedure for the preparation of layer-by-layer stacked graphite-reinforced carbon (GrC) fiber electrodes.

Figure 2 provides a schematic representation of the capacitive deionization set-up.

Figure 3 A & B) FESEM images of layer-by layer stacked graphite reinforced carbon fiber. The white arrow in figure B shows the presence of graphite flakes. The inset in figure B represents the single layer graphenic carbon (b), C) TEM image, the inset c1 represents the Raman spectrum of the material and c2 represents the HRTEM image of graphenic carbon, D) XPS survey spectrum of the material and the inset shows the deconvoluted C1s spectrum.

Figure 4 A) Electro-adsorption/desorption curve of the graphite-reinforced carbon fiber electrode for a single cycle. The electrolyte present is NaCl measured at room temperature. B)

EDS spectra of i) positive and ii) negative terminals after single adsorption cycle. The corresponding SEM images (a1 and b1) along with the elemental maps (a2 and b2) are shown in the inset. C) XPS survey spectrum of the material after single adsorption cycle, a) positive and b) negative terminals. The inset shows the deconvoluted XPS spectrum of Cl2p and Na1s.

5 **Figure 5** A) Electro-adsorption/desorption cycles of the material (up to four cycles). B) XPS spectrum of regenerated positive terminal after 10th cycle showing the presence of carbon and oxygen only. The inset shows the deconvoluted C1s and O1s spectrum. C & D) EDS spectra in the inset show the SEM image and the corresponding elemental maps for carbon, oxygen and respective adsorbed ions. The electrolyte used in all cases was NaCl.

10 **Figure 6** provides plot of CDI performance of graphite reinforced carbon fiber electrode in the mixed negative ions ($\text{Cl}^- > \text{NO}_3^- > \text{F}^- > \text{SO}_4^{2-}$) system (A). Raman spectra of graphite reinforced carbon fiber electrode before and after electro-adsorption of positive electrode (B). Plot of desorption capability of electrode in 1st and 10th cycle (C). SEM images of before and after 5 days growth of biofilms of *Pseudomonas putida* on commercial electrode (D(i,ii)) and graphite reinforced-carbon fiber electrode (D(iii,iv)).

Figure 7 illustrates EDS spectrum of the layer-by-layer stacked carbon-graphite electrode before SiO_2 etching. Inset: Its corresponding SEM image and elemental mapping images.

Figure 8 illustrates EDS spectrum of the layer-by-layer stacked carbon-graphite electrode after etching SiO_2 . Inset: SEM and Elemental mapping images.

20 **Figure 9** illustrates N_2 adsorption-desorption isotherms of graphite-reinforced carbon fiber electrode.

Figure 10 illustrates electro-adsorption and desorption performance of the graphite-reinforced carbon fiber electrode in NaCl solution. EDS spectrum and their elemental mapping images of the regenerated positive terminal carbon-graphite electrode (after first cycle). *Note: Aluminum comes from the SEM sample stubs.*

Figure 11 illustrates electro-adsorption and desorption performance of the graphite-reinforced carbon fiber electrode in NaCl solution. EDS spectrum and their elemental mapping images of the regenerated negative terminal carbon-graphite electrode (after first cycle).

30 **Figure 12** illustrates electro-adsorption and desorption performance of the graphite-reinforced carbon fiber electrode in NaCl solution. EDS spectrum and their elemental mapping images of

the regenerated positive terminal carbon-graphite electrode (after ten consecutive cycle). *Note: Aluminum comes from the SEM sample stubs.*

Figure 13 illustrates electro-adsorption and desorption performance of the graphite-reinforced carbon fiber electrode in NaCl solution. EDS spectrum and their elemental mapping images of the regenerated negative terminal carbon-graphite electrode (after ten consecutive cycle).

Figure 14 provides a plot of CDI results of electro-adsorption and desorption performance of the graphite-reinforced carbon fiber electrode in different charged species ie., Na^+ , Mg^{2+} and Fe^{3+} .

Figure 15 illustrates electro-adsorption and electro-desorption performance of the graphite-reinforced carbon fiber electrode in MgCl_2 solution. EDS spectrum and their elemental mapping images of the negative terminal after electro-adsorption on the carbon-graphite electrode. *Note: Calcium is from the water used.*

Figure 16 illustrates electro-adsorption and desorption performance of the graphite-reinforced carbon fiber electrode in MgCl_2 solution. EDS spectrum and their elemental mapping images of the positive terminal after electro-adsorption the carbon-graphite electrode.

Figure 17 illustrates electro-adsorption and desorption performance of the graphite-reinforced carbon fiber electrode in FeCl_3 solution. EDS spectrum and their elemental mapping images of the negative terminal after electro-adsorption on the carbon-graphite electrode.

Figure 18 illustrates electro-adsorption and desorption performance of graphite reinforced carbon fiber electrode in FeCl_3 solution. EDS spectrum and elemental maps of the positive terminal after electro-adsorption on the carbon-graphite electrode.

Figure 19 illustrates CDI performance of graphite reinforced carbon fiber electrode in the mixed negative ions (Cl^- , F^- , NO_3^- , SO_4^{2-}) system. EDS spectrum and elemental maps of the negative terminal after electro-adsorption on the porous carbon-graphite electrode. *Note: Aluminum comes from the SEM sample stubs.*

Figure 20 illustrates CDI performance of graphite reinforced carbon fiber electrode in the mixed negative ions (Cl^- , F^- , NO_3^- , SO_4^{2-}) system. EDX spectrum and elemental maps of the positive terminal after electro-adsorption on the porous carbon-graphite electrode. *Note: Aluminum comes from the SEM sample stubs.*

Referring to the drawings, the embodiments of the present invention are further described. The figures are not necessarily drawn to scale, and in some instances the drawings have been exaggerated or simplified for illustrative purposes only. One of ordinary skill in the art

may appreciate the many possible applications and variations of the present invention based on the following examples of possible embodiments of the present invention.

DETAILED DESCRIPTION OF THE INVENTION

5

The present invention describes a graphite reinforced-cellulose (GrC) derived 3D mesoporous fibrous carbon electrode for capacitive deionization.

Some embodiments of the present invention relate to a capacitive deionization apparatus having improved desalination efficiency.

10

Another aspect of the invention relates to synthesis of reinforced-cellulose (GrC) derived carbon electrode by a layer-by-layer method.

15

Some embodiment of the present invention relate to electro-adsorption of NaCl on the graphite reinforced-cellulose (GrC) electrode which reached equilibrium quickly (within 90 min) and the adsorbed salts were released swiftly (in 40 min) back into the solution, during reverse the terminal.

Another aspect of the invention relates to GrC electrode with highest electro-adsorption capacity of 13.1 mg/g at a cell potential of 1.2 V, with excellent recyclability and complete regeneration.

20

Another embodiment of the present invention relate to electrode has a high tendency for removal of specific anions, such as fluoride, nitrate, chloride and sulphate from water in the following order: $Cl^- > NO_3^- > F^- > SO_4^{2-}$.

Other aspect of the invention relate to surface morphology of graphenic carbon fiber electrode provides resistance against bacterial adhesion and proliferation but not limited to biofouling and biofilm formation by *Pseudomonas putida*.

25

According to the embodiments of the present invention, the graphite reinforced-cellulose (GrC) derived carbon fiber electrode provides uniform conductivity throughout the electrode with fast electro-adsorption, rapid desorption and extended reuse making the electrode affordable for capacitive desalination of brackish water in resource limited settings.

30

It may be appreciated by those skilled in the art that the drawings, examples and detailed description herein are to be regarded in an illustrative rather than a restrictive manner.

Some embodiments of the present invention describe the method and preparation of layer-by-layer assembly of graphite reinforced-carbon electrode as follows;

The following method offered by way of illustration and not by way of limitation. The disclosures of all citations in the specification are expressly incorporated herein by reference.

Materials and method

5 Chemicals

Graphite flakes were a gift sample from Tamil Nadu Minerals Limited (TAMIN) and tissue papers were purchased from a local market in Chennai. Tetraethyl orthosilicate (TEOS) and 3-aminopropyltriethoxysilane (APTES) were purchased from Sigma–Aldrich and used as such. Unless otherwise specified, all the reagents used were of analytical grade and the solutions
10 were prepared using deionized water.

Preparation of layer-by-layer assembly of graphite reinforced-carbon electrode

The typical procedure for the preparation of a layer-by-layer assembly of a graphite reinforced-carbon (GrC) electrode was as follows (see Figure 1). First, 5 mg of graphite
15 (TAMIN) powder was coated on a single piece of tissue paper (size 5 x 5 cm and thickness of 0.2 mm) and then 300 μ L of TEOS:APTES mixture (ratio 1:0.5) was sprayed on it. This process was repeated for each layer (total 50 layers were prepared). Next, the entire set of graphite coated tissue paper layers were stacked on one above another and was pressed for 5 min (at 5 ton load) by a press. It was further dried at 60 $^{\circ}$ C for 3 h, which was followed by carbonization under
20 nitrogen atmosphere at 700 $^{\circ}$ C for 3 h. After carbonization, silica was etched out from the stacked GrC electrode by aqueous NaOH (1 mM) for 3h to generate pores. Finally, the electrode was washed with water several times until the pH of the mother liquor reached 7 and then dried overnight at 60 $^{\circ}$ C to remove water.

25 Capacitive deionization set-up

The laboratory-scale CDI batch reactor consisted of a single pair of GrC electrodes and a pair of current collectors, as shown in Figure 2. The current collectors were made of graphite rods and the electrodes were held at a spacing of \sim 0.2 mm by a piece of nylon membrane. Power was supplied to the cell by connecting the current collectors to a direct-current (DC) Test-tronic
30 30B DC power supply with a voltage range of 0-5 V and a current range of 0-1 A. The conductivity was measured at the cell exit stream by using a conductivity meter (cyberscan PCD

650 Eutech instrument). Approximate volume of the solution in the cell was 80 mL, which was maintained in the system. The temperature of the solution was kept at ~25 °C. Regeneration of the electrodes was carried out by reversing the terminal of the electrodes.

5 **Biofilm formation**

Monoculture biofilms of *Pseudomonas putida* were grown on the surface of the electrodes (a commercial electrode used for capacitive deionization and GrC). The protocol for the bio-film is reported elsewhere [*Trends Microbiol* 9, 222-227]. A few selected electrodes were immersed in 20 mL of a synthetic medium, inoculated with 10^8 colony forming units (CFU) of *Pseudomonas putida*. The biofilm was allowed to grow for 5 days while replenishment of the medium was done at an interval of 48 h. The electrodes after biofilm growth were rinsed in distilled water and air dried for 24 h. The surfaces were sputtered with gold to increase their electrical conductivity before imaging. Scanning electron microscopic studies were performed using a FEI QUANTA-200 SEM operated at 12.5kV.

15

Characterization studies

Morphological studies of the electrode surface, elemental analysis and elemental mapping were carried out using a Scanning Electron Microscope (SEM) equipped with Energy Dispersive Analysis of X-rays (EDAX or Energy Dispersive Spectroscopy, EDS) (FEI Quanta 200). The High Resolution Transmission Electron Microscopy (HRTEM) images of the electrodes were obtained with an instrument, JEM 3010 (JEOL, Japan) which was operated at 200 keV (to reduce beam induced damage) and the samples were drop-cast on carbon-coated copper grids and allowed to dry under ambient conditions. X-ray Photoelectron Spectroscopy (XPS) measurements were performed using ESCA Probe TPD of Omicron Nanotechnology with polychromatic Mg K α as the X-ray source ($h\nu = 1253.6$ eV) and the binding energy was calibrated with respect to C1s at 284.5 eV. Flowsorb II 2300 Micrometrics surface area analyzer was employed for measuring the surface area, pore volume and pore diameter of the samples. Total sodium and chloride concentrations in the water were estimated using inductively coupled plasma spectroscopy (ICP-MS) (Perkin Elmer NexION 300 ICP-MS) and Ion chromatography (Metrohm 883 Basic IC plus), respectively. Raman spectra were obtained with a WITec GmbH,

30

Alpha-SNOM alpha 300 S confocal Raman microscope having a 532 nm laser as the excitation source.

Results and Discussion

5 Characterization of layer-by-layer stacked assembly of graphite reinforced-carbon (GrC) electrode

To investigate the morphology of the GrC electrode, FESEM and HRTEM images were analyzed. Figure 3A, B and C show that the prepared GrC electrodes are collectively intertwined in a unique fiber-like morphology with a thickness of 4–5 μm and a length of ten to several hundred micrometers. The graphite reinforcement into the consecutively stacked layer-by-layer assembly of carbon fiber is also evident from Figure 3A and 3B marked in white arrows. This arrangement established an effective way for improving conductivity as well as mechanical strength. The material proved to be superior to similar carbon-carbon composites [Carbon 1972,10, 383-390; Carbon 1987,25, 163-190; Mater. Des. 1997,18, 11-15; Carbon 1988,26, 333-337]. The elemental mapping confirmed the presence of silica in the initial material (Figure 7). Figure 8 shows the complete etching of silica from the parent material, which led to the characteristic porosity of the GrC electrode. Furthermore, the Raman spectrum of the assembly in inset C₁ in Figure 3C clearly shows that the material is graphenic in nature. The spectrum is composed of a primary in-plane vibrational mode at 1580 cm^{-1} (G band) and a second order overtone of a different in-plane vibration at 2690 cm^{-1} (2D band) and a defect band at 1350 cm^{-1} (D band) [J. Hazard. Mater. 2013, 246–247, 213-220; ACS Nano 2013, 8, 234-242; J. Mater. Chem. A 2013, 1, 12334-12344]. This graphenic nature of the single carbon fiber represents multilayer graphene as shown in HRTEM image in the inset of Figure 3C (c2). X-ray photoelectron survey spectrum of GrC electrode is shown in Figure 3D. It shows the presence of carbon and oxygen as the only elements. The deconvoluted C 1s XPS (Inset in Figure 3D) spectrum shows the presence of C=C at 284.6 eV and two "oxide" peaks that are shifted to higher binding energy by 1.0 eV and 1.5 eV, respectively. The first oxide peak is assigned to a carbon atom in alcohol (C-OH) or ether (C-O-C) groups. The second type of oxide corresponds to a C atom in carbonyl (C=O) type groups.

30 Structural properties (surface area and pore characteristic) and electrical conductivity have a major effect on the CDI performance of carbon materials. Therefore, the specific surface

areas and the pore size distributions of the GrC electrode were measured using the BET and BJH methods. The nitrogen adsorption-desorption isotherms observed for the GrC electrode are shown in Figure 9. The calculated BET surface area and pore volume of the prepared samples are $598 \text{ m}^2 \text{ g}^{-1}$ and $0.358 \text{ cm}^3 \text{ g}^{-1}$, respectively. The N_2 adsorption increased for $P/P_0 > 0.1$ owing to capillary condensation and multilayer adsorption of N_2 and the typical type-IV isotherm with H4 hysteresis loops indicate that the layer-by-layer assembly of carbon electrode is mesoporous in nature [The J. Phys. Chem. C **2011**, *115*, 17068-17076; J. Mater. Chem. A **2013**, *1*, 11778-11789; J. Mater. Chem. A **2013**,*1*, 12334-12344]. The BET isotherm results suggest that the GrC electrodes expected to be a potential candidate for salt adsorption from water in CDI.

10

CDI performance of the GrC electrode

The CDI efficiency of the graphite reinforced-carbon electrode was evaluated using NaCl solution at room temperature by using a single CDI cell (as depicted in Figure 2) with an applied voltage of 1.2 V. Generally, water with Total Dissolved Solids (TDS) higher than 500 mg/L is not considered suitable for consumption [Sep. Purif. Technol. **2010**,*71*, 70-75]. The present invention chose NaCl concentrations of 500 mg/L to test the CDI performance of these electrode materials. In Figure 4A, the NaCl electro-adsorption and electro-desorption profiles of the electrode are plotted as a function of time. It is noticeable from the figure that the concentration of NaCl (500 mg/L) in the solution decreases gradually with time and reaches equilibrium. In comparison, when the potential was reversed, a rapid increase in NaCl concentration in solution occurs, which later stabilizes. One can further deduce from the electro-adsorption and electro-desorption profiles that ~30% of NaCl is adsorbed in the first step, which is completely desorbed from the electrode on reversing the potential [Energy Environ. Sci. **2013**, *6*, 3700-3712; RSC Adv. **2014**, *4*, 64634-64642; J. Mater. Chem. A **2013**, *1*, 11778-11789; J. Mater. Chem. A **2013**,*1*, 12334-12344]. This implies that the present invention porous carbon-graphite hybrid electrode can be regenerated efficiently.

15

20

25

The NaCl electro-adsorption capacity (q_e) of the electrodes is calculated from the following equation:

$$q_e = \frac{(c_0 - c_f)V}{W} \quad (1)$$

where C_0 and C_f are the initial and final NaCl concentrations (in mg/L) in solution, respectively, V is the volume (in mL) of the NaCl solution used, and W is the mass (in g) of the active material in the working electrode. The q_e of the graphite reinforced-carbon electrode was evaluated as 13.1 mg/g. Notably, the NaCl electro-adsorption capacity of the carbon-graphite hybrid electrode in this work is much higher than that of other recently reported CDI electrode materials, e.g. 0.731 mg/g for graphene incorporated-mesoporous carbon sheet [*Energy Environ. Sci.* **2012**, *5*, 9511-9519; *J. Mater. Chem. A* **2013**, *1*, 6335-6341; *J. Mater. Chem. A* **2014**, *2*, 3484-3491; *J. Mater. Chem. A* **2013**, *1*, 11001-11010; *Nanoscale* **2012**, *4*, 5440-5446; *J. Mater. Chem.* **2012**, *22*, 23835-23844; *Nano Lett.* **2012**, *12*, 839-843].

Fast electro-adsorption rate is also an important criterion responsible for allowing practical applications of CDI electrode materials. Various carbon based materials require several hours to reach their electro-adsorption equilibrium [*J. Mater. Chem. A* **2013**, *1*, 11001-11010; *J. Mater. Chem.* **2012**, *22*, 23835-23844]. From the time dependent desalination behavior of the GrC electrode in Figure 4A it is evident that the electro-adsorption of 500 mg/L NaCl reaches equilibrium quickly within 90 min, and the adsorbed salts are swiftly released back into the solution in 40 min during discharge compared to *Li et al.* reported around 120 mins for electro-adsorption [*Carbon* **2009**, *47*, 775-781].

Elemental mapping and EDS analysis of the positive and negative electrodes are shown in Figure 4B and Figure 10 and 11. It clearly shows that the graphite reinforced-carbon electrodes have the capacity to remove salts from brackish water and get regenerated quickly. The XPS spectra of the positive and negative electrodes after application of potential are presented in Figure 4C. In comparison with Figure 3D, new peaks due to sodium and chloride ions adsorbed on the negative and positive electrode, respectively can be seen in the spectra. Interestingly, adsorption of these ions did not alter the binding energies of the carbon and oxygen peaks. This demonstrates that electro-adsorption of Na^+ and Cl^- ions on the electrodes is via physisorption alone [*J. Hazard. Mater.* **2013**, *246-247*, 213-220; *Small* **2013**, *9*, 273-283].

Studies were performed to investigate the reversibility of the GrC electrode during adsorption and regeneration. Figure 5A shows the ratio of initial concentration (C_0) to concentration at a time t (C_t) over several consecutive cycles. The symmetrical nature of the electro-adsorption (deionization) and desorption (regeneration) curves is characteristic of first order kinetics associated with ion uptake and removal by the hybrid electrode [*Chem. Eng. J.*

2013, 223, 704-713; *J. Hazard. Mater.* **2012**, 213–214, 491-497]. The surface of electrodes was characterized using XPS as shown in Figure 5B. Interestingly, there was no feature in the XPS spectrum corresponding to the negative and positive ions, and no shift in the binding energy of carbon and oxygen was observed. The EDS elemental mapping of anode and cathode after tenth adsorption cycle is shown in Figure 5C and 5D and the corresponding EDS maps of the regenerated electrodes are shown in Figure 12 and 13. This study confirms that the GrC electrode maintains its adsorption and desorption capacity even after ten consecutive cycles. These results exhibit the high electro-adsorption capacity and a fast and reversible electro-adsorption/desorption.

10 The electro-adsorption capacity is known to strongly depend on the surface properties, such as surface area, pore microstructure and pore size distribution and as well as solution state properties of the electrode material [*Energy Environ. Sci.* **2013**, 6, 3700-3712; *RSC Adv.* **2014**, 4, 64634-64642; *J. Mater. Chem. A* **2013**, 1, 11778-11789; *J. Mater. Chem. A* **2013**, 1, 12334-12344; *J. Hazard. Mater.* **2012**, 213–214, 491-497]. The layer-by-layer assembly of the present
15 invention GrC electrodes increases the mass transfer of ions into the pores, ion electro-adsorption and energy storage in the electrical double layer of the electrode. This consequently reduces the mass transport resistance of salt ions inside the electrode as well as between the electrode and saline water. This structural feature gives rise to a high electro-adsorption rate of the GrC electrodes and therefore, leads to excellent CDI performance.

20 The electro-adsorption capacity of the GrC electrodes was further investigated with respect to the effect of cation charge and size. To this end solutions of $MgCl_2$ and $FeCl_3$, each at an initial concentration of 500 ppm, were selected. The electro-adsorption and electro-desorption profiles of the GrC electrode for these solutions are compared with those of $NaCl$ (500 ppm) in Figure 14. The concentrations of MCl_x solutions decreases with respect to time and varies in the
25 order of $Fe^{3+} > Mg^{2+} > Na^+$. It is understandable that the ionic charge, ionic radii and hydrated radii of different cations may play a major role in governing the electro-adsorption process. The hydrated radius of Fe^{3+} is the largest while that of Na^+ is the smallest in these cations, based on which the electro-adsorption preference should exhibit an opposite trend. The above order can instead be explained in terms of charge of the cations; as cations with higher charge will be more
30 easily adsorbed on the electrode surface on application of a potential at the electrodes. Thus, the trivalent Fe^{3+} ion is most effectively removed, followed by the bivalent Mg^{2+} ion, and then the

univalent Na^+ ion [*J. Mater. Chem.* **2012**, *22*, 6603-6612; *J. Hazard. Mater.* **2012**, *213–214*, 491-497]. The GrC electrodes used in this study have a layer-by-layer assembly which allows the cations to move easily over the carbon-graphite electrode through the pores. This is confirmed from EDS coupled with elemental mapping analysis (Figure 15-18).

5 Anion contamination of both surface water and ground water is well documented [*PNAS* **2014**, *111*, 3245-3250; *Nature* **2008**, *452*, 301-310; *PNAS* **2013**, *110*, 8459-8464]. To test the effectiveness of the present invention electrode for electro-adsorption of anions, several experiments were carried out using a solution containing different anions (such as SO_4^{2-} , Cl^- , NO_3^- and F^-). The initial concentration of each of the selected anions was fixed at 50 ppm. About
10 2 mL aliquot of the analyte was withdrawn at regular intervals and an analysis via ion chromatography was performed. Figure 6A shows that for each anion the concentration decreases with increase in time, indicating that they are adsorbed on the GrC electrode. These results were further confirmed through Raman spectroscopy (Figure 6B) and elemental mapping (Figure 19 and 20). Raman spectra evidently indicate the presence of symmetric N-O and S-O
15 stretching vibrations at 1056 cm^{-1} and 990 cm^{-1} for nitrate and sulfate, respectively [*J. Chem. Phys.* **1985**, *82*, 1732-1740]. These features appeared clearly in the positive carbon-graphite electrode after electro-adsorption. Elemental mapping of positive and negative electrodes provide further evidence confirming electro-adsorption.

It can also be noticed from the adsorption profiles in Figure 6A that at a given time t , the
20 measured anion concentration variation in solution follows the order: $\text{Cl}^- > \text{NO}_3^- > \text{F}^- > \text{SO}_4^{2-}$. Size of the hydrated radii of these anions decreases as $\text{SO}_4^{2-} > \text{F}^- > \text{Cl}^-$, NO_3^- . Anions with smaller hydrated radii can pass through the pores and arrive at the electrode surface more easily [*J. Hazard. Mater.* **2012**, *213–214*, 491-497; *Curr. Phys. Chem.* **2011**, *1*, 16-26]. As a result, higher fractions of Cl^- and NO_3^- are removed than the other two anions. Finally, the recyclability of the
25 GrC electrodes when treating water containing a mixture of anions was tested. The present invention found negligible difference between the first and tenth cycles (Figure 6C) which indicate that the electrodes were completely regenerated even after ten cycles.

Biofouling of electrodes is a major issue impeding their utilization in the CDI process and is detrimental to their practical applications [*Prog. Mater. Sci.* **2013**, *58*, 1388-1442]. Though
30 employing conventional biofouling control methods during capacitive desalination process can reduce biofouling of the electrodes, they also generate harmful byproducts requiring additional

treatment [*Membranes* **2012**, *2*, 804-840]. In this context, the present invention tested the effect of biofouling with *Pseudomonas putida* on the graphite reinforced-carbon fiber electrode. The SEM results (Figure 6D) showed that in comparison with a commercially available electrode, the present invention graphite reinforced-carbon fiber electrode has an enhanced resistance to biofouling. This could be due to the graphenic nature of carbon fibers, [*Nanoscale* **2014**, *6*, 1879-1889] which have been individually proven to be effective antibacterial agents. The fiber-like surface morphology of the electrode could also provide it resistance against bacterial adhesion and proliferation. This is understandable because the surface charge of the carbon fiber-like structure may effectively repel bacteria from initial attachment on the GrC fiber electrode, thereby making it an effective material for long-term use [*Membranes* **2012**, *2*, 804-840; *Nanoscale* **2014**, *6*, 1879-1889; *J. Mater. Chem.* **2010**, *20*, 4567-4586].

15

20

We claim:**CLEAN COPY**

1. A graphite reinforced-cellulose derived carbon fiber (GrC) electrode prepared via layer-by-layer stacking method for capacitive desalination, wherein the said electrode increases the conductivity with high electro-adsorption capacity of 13.1 mg/g at a cell potential of 1.2 V and, with excellent recyclability and complete regeneration.
2. The electrode as claimed in claim 1, wherein electro-adsorption of NaCl on the graphite reinforced-cellulose derived carbon fiber (GrC) electrode reached equilibrium within 90 minutes and the adsorbed salts were released within 40 minutes back into the solution during reversibility.
3. The electrode as claimed in claim 1, wherein the electrode has tendency for removal of specific anions, such as fluoride, nitrate, chloride and sulfate from water in the following order: $\text{Cl}^- > \text{NO}_3^- > \text{F}^- > \text{SO}_4^{2-}$.
4. A method of preparing cellulose derived carbon fiber electrode in layer-by-layer stacking method for capacitive desalination involving:
 - a. graphite powder coated on a single piece of tissue paper followed by spraying tetraethyl orthosilicate (TEOS): 3-aminopropyltriethoxysilane (APTES) mixture and repeating this process for 50 layers;
 - b. graphite coated tissue paper layers stacked one above another and dried at 60°C for 3 h, which was followed by carbonization under nitrogen atmosphere at 700 °C for 3 h;
 - c. after carbonization silica was etched out from the stacked GrC electrode by aqueous NaOH 1 mM for 3h to generate pores; and
 - d. finally, the electrode was washed with water several times until the pH of the mother liquor reached 7 and then dried overnight at 60°C to remove water.
5. The electrode as claimed in claim 1 and 5, wherein layer-by-layer assembly allows the cations to move easily over the carbon-graphite electrode through the pores resulting in high electro-adsorption performance.
6. The electrode as claimed in claim 1 and 5, wherein the surface morphology of the electrode provide resistance against bacterial adhesion and proliferation but not limited to biofouling and biofilm formation by *Pseudomonas putida*.
7. The electrode as claimed in claim 1 and 5, wherein the electrode provides uniform conductivity with fast electro-adsorption, rapid desorption and extended reuse making

the electrode affordable for capacitive desalination of brackish water in resource limited settings.

8. The electrode as claimed in claim 1 and 5 wherein the carbon fibers are modified chemically or physically by the treatment with acids, bases or chemicals to vary their surface properties.

Dated at Chennai this October 26, 2019

Signature: 

D. Moses Jeyakaran
Advocate & Patent Agent
IN/PA — 369

CELLULOSE DERIVED GRAPHENIC FIBERS FOR CAPACITIVE DESALINATION OF BRACKISH WATER AND PREPARATION METHOD OF THE ELECTRODE THEREOF

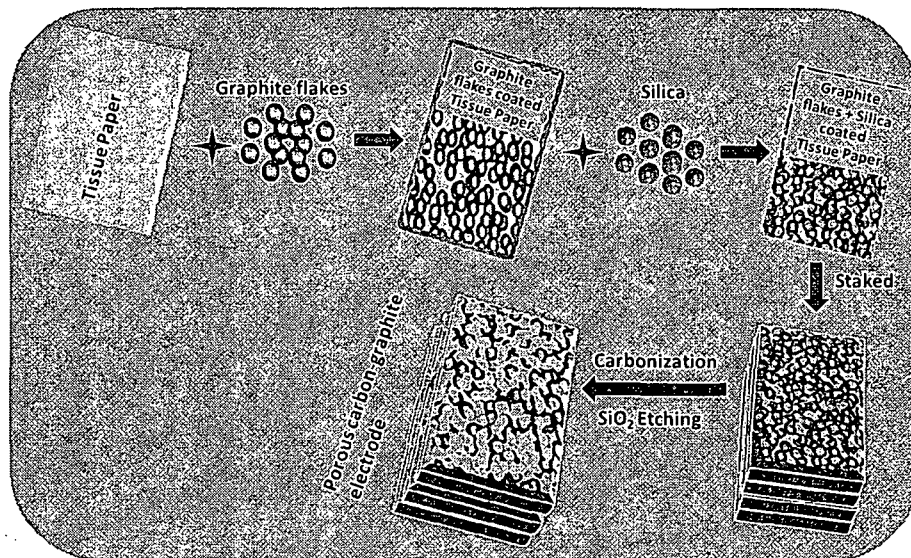


FIGURE 1

Signature:

D. Moses Jeyakaran
Advocate & Patent Agent
IN/PA — 369

31 JUL 2015

10

15

ORIGINAL

25

30

35

3951 /CHE/ 2015

5 CELLULOSE DERIVED GRAPHENIC FIBERS FOR CAPACITIVE DESALINATION
OF BRACKISH WATER AND PREPARATION METHOD OF THE ELECTRODE
THEREOF

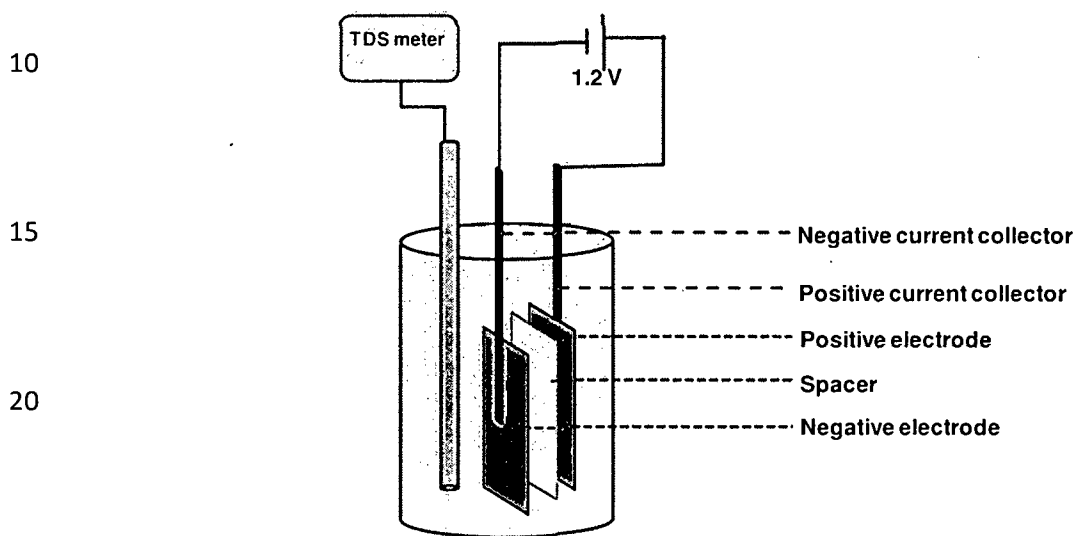


FIGURE 2

Signature: 

D. Moses Jeyakaran
Advocate & Patent Agent
IN/PA — 369

CELLULOSE DERIVED GRAPHENIC FIBERS FOR CAPACITIVE DESALINATION
OF BRACKISH WATER AND PREPARATION METHOD OF THE ELECTRODE
THEREOF

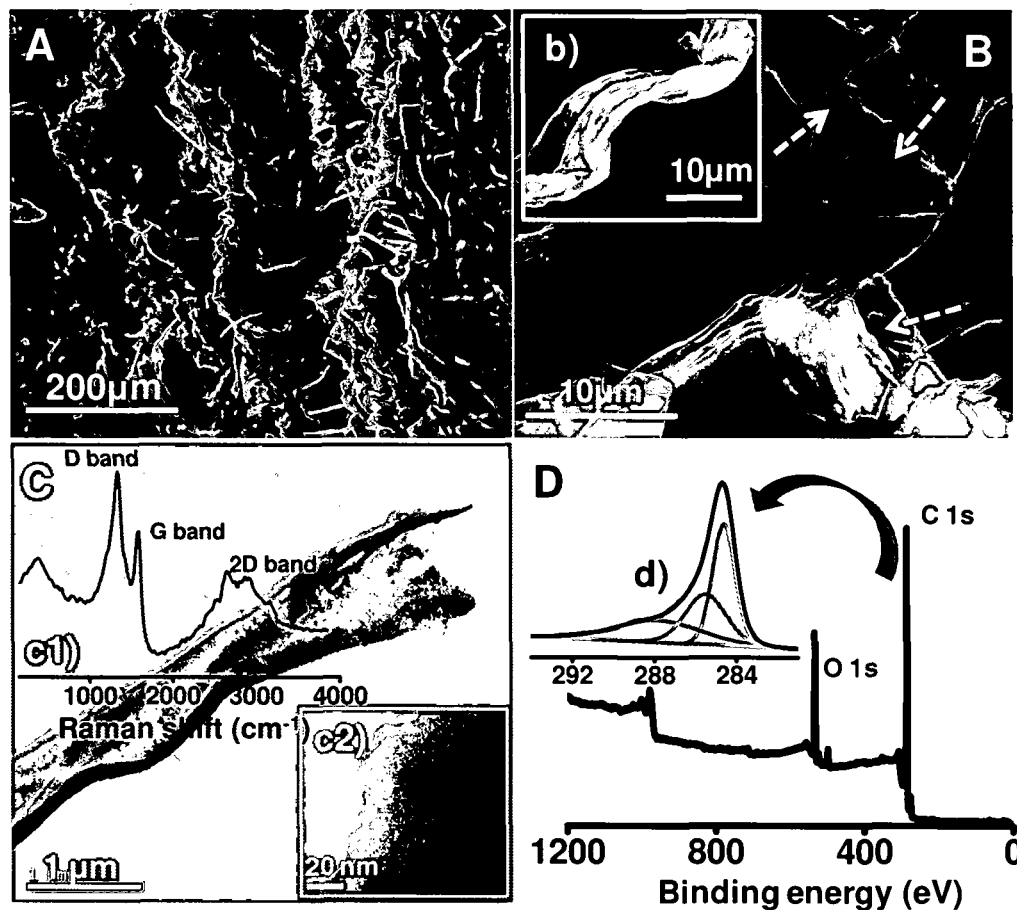


FIGURE 3

Signature:

D. Moses Jeyakaran
Advocate & Patent Agent
IN/PA — 369

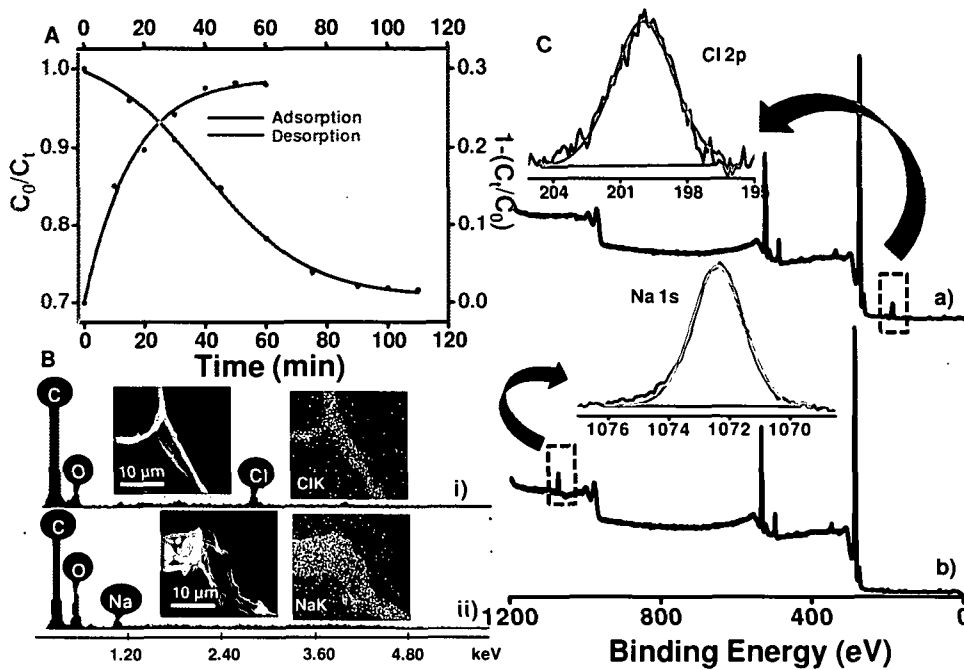
CELLULOSE DERIVED GRAPHENIC FIBERS FOR CAPACITIVE DESALINATION OF BRACKISH WATER AND PREPARATION METHOD OF THE ELECTRODE THEREOF

5

10

15

20



25

FIGURE 4

30

Signature:

D. Moses Jeyakaran
 Advocate & Patent Agent
 IN/PA — 369

CELLULOSE DERIVED GRAPHENIC FIBERS FOR CAPACITIVE DESALINATION OF BRACKISH WATER AND PREPARATION METHOD OF THE ELECTRODE THEREOF

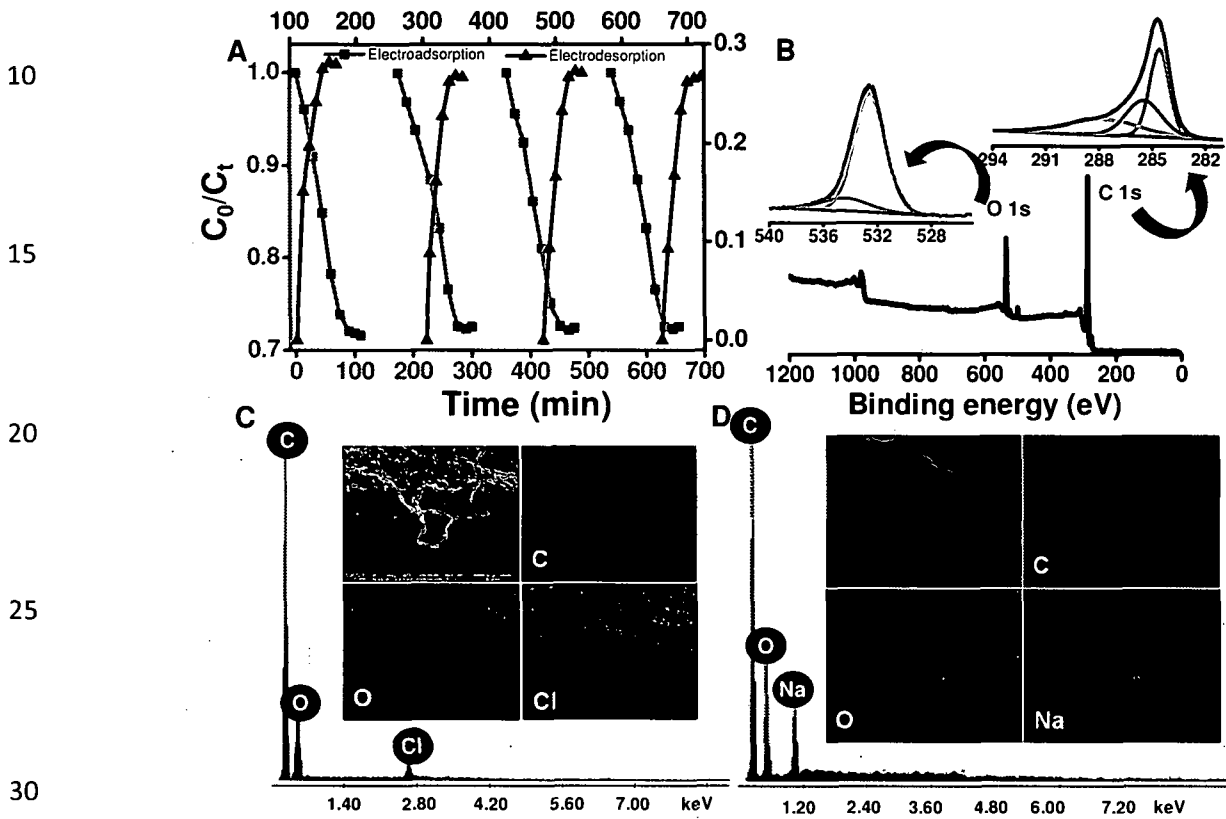


FIGURE 5

Signature:

D. Moses Jeyakaran

D. Moses Jeyakaran
Advocate & Patent Agent
IN/PA — 369

CELLULOSE DERIVED GRAPHENIC FIBERS FOR CAPACITIVE DESALINATION
 OF BRACKISH WATER AND PREPARATION METHOD OF THE ELECTRODE
 THEREOF

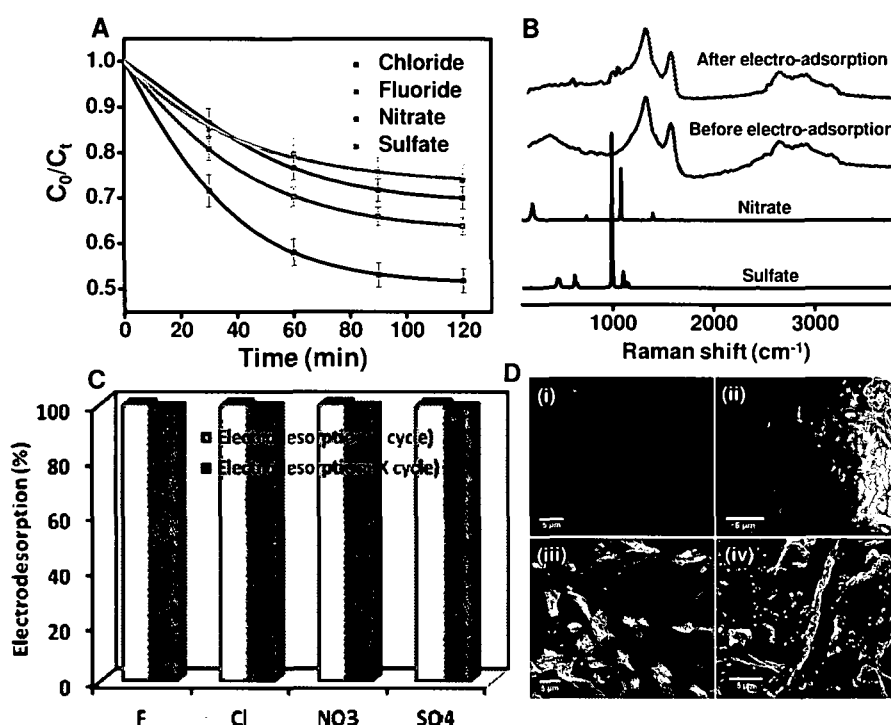
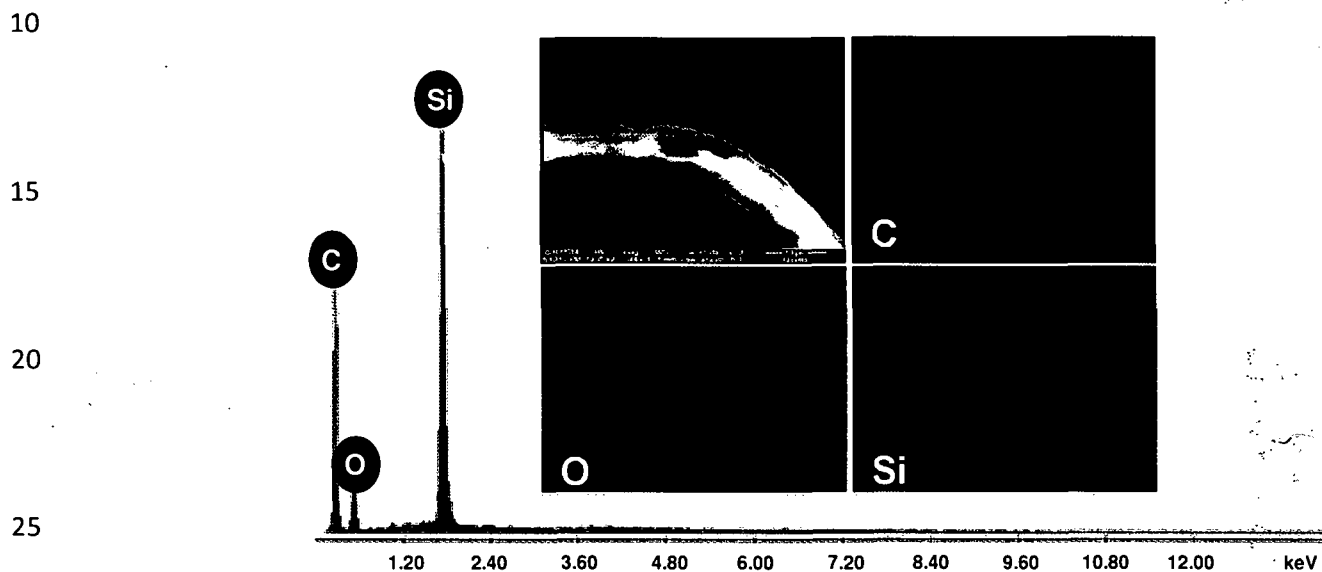


FIGURE 6

Signature: *D. Moses Jeyakaran*

D. Moses Jeyakaran
 Advocate & Patent Agent
 IN/PA — 369

5 CELLULOSE DERIVED GRAPHENIC FIBERS FOR CAPACITIVE DESALINATION
OF BRACKISH WATER AND PREPARATION METHOD OF THE ELECTRODE
THEREOF



30 FIGURE 7

35 Signature:

D. Moses Jeyakaran
Advocate & Patent Agent
IN/PA — 369

40

5 CELLULOSE DERIVED GRAPHENIC FIBERS FOR CAPACITIVE DESALINATION
OF BRACKISH WATER AND PREPARATION METHOD OF THE ELECTRODE
THEREOF

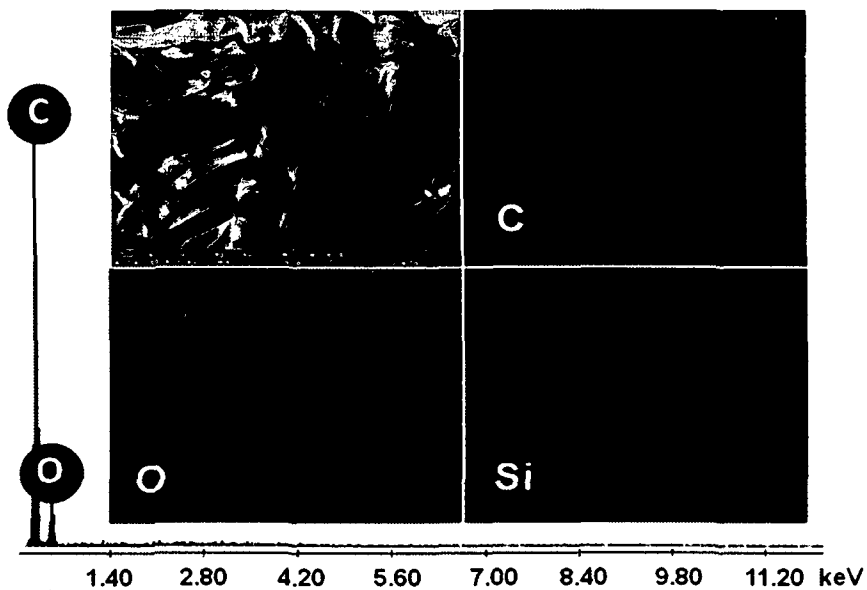


FIGURE 8

Signature: *D. Moses Jeyakaran*

D. Moses Jeyakaran
Advocate & Patent Agent
IN/PA — 369

CELLULOSE DERIVED GRAPHENIC FIBERS FOR CAPACITIVE DESALINATION
OF BRACKISH WATER AND PREPARATION METHOD OF THE ELECTRODE
THEREOF

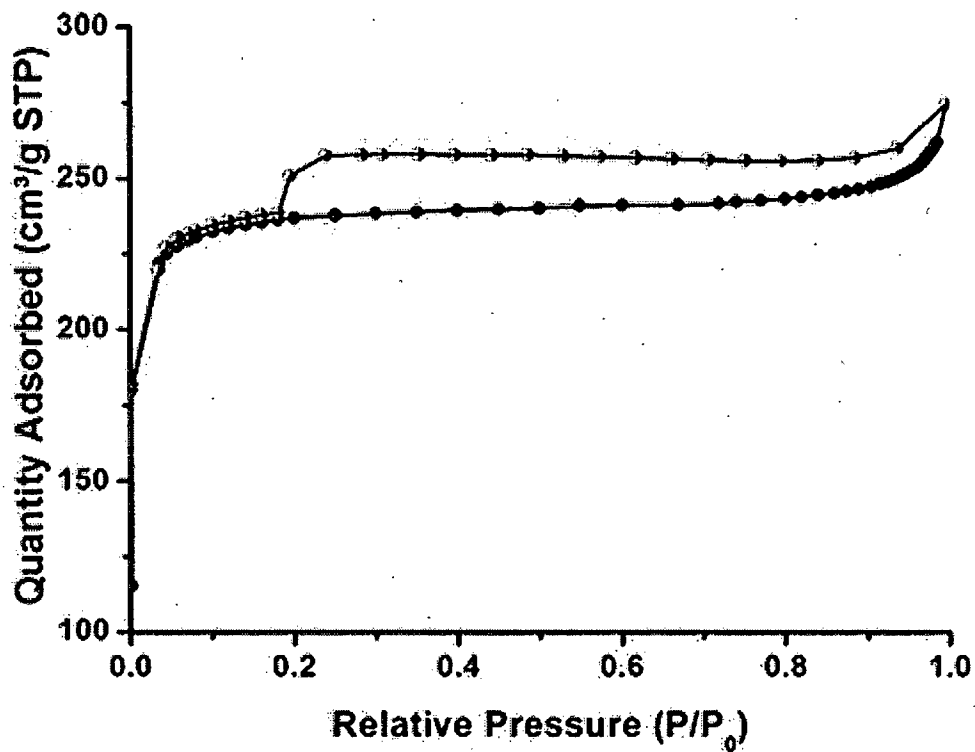
10

15

20

25

30



35

FIGURE 9

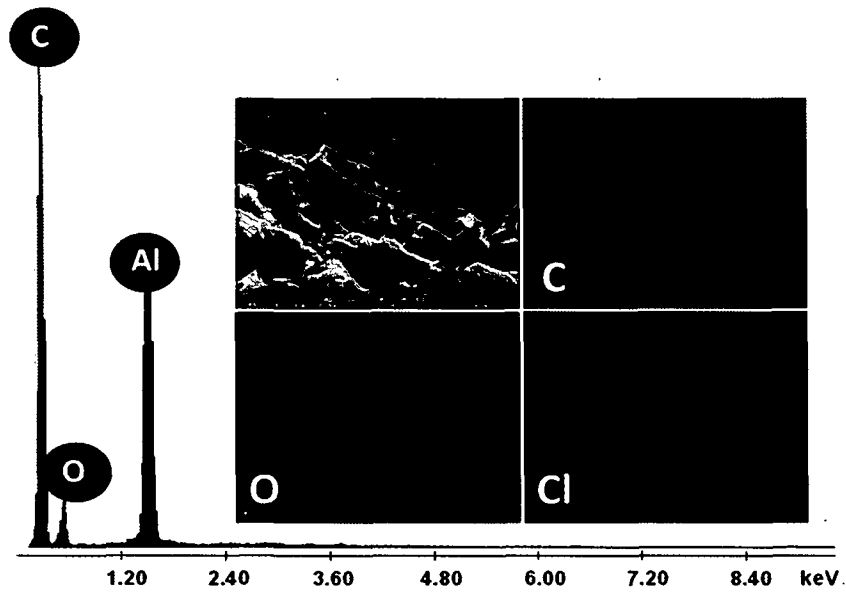
40

Signature:

D. Moses Jeyakaran
Advocate & Patent Agent
IN/PA — 369

45

5 CELLULOSE DERIVED GRAPHENIC FIBERS FOR CAPACITIVE DESALINATION
OF BRACKISH WATER AND PREPARATION METHOD OF THE ELECTRODE
THEREOF

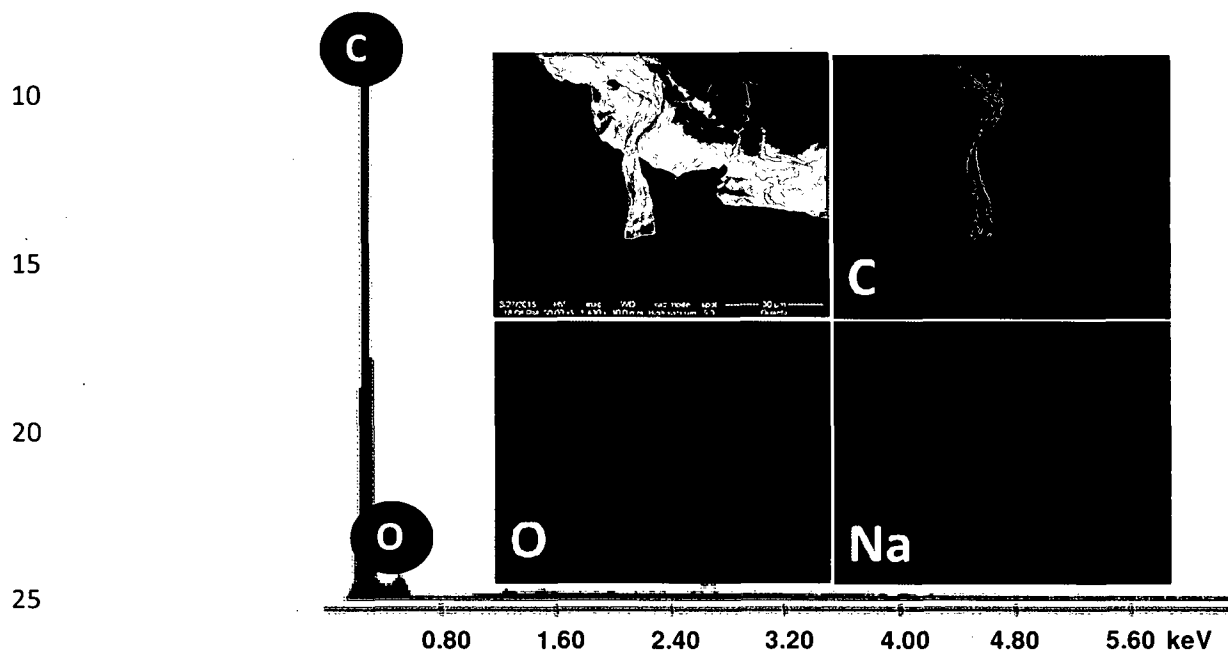


10
15
20
FIGURE 10

Signature:

D. Moses Jeyakaran
Advocate & Patent Agent
IN/PA — 369

5 CELLULOSE DERIVED GRAPHENIC FIBERS FOR CAPACITIVE DESALINATION
OF BRACKISH WATER AND PREPARATION METHOD OF THE ELECTRODE
THEREOF



30 FIGURE 11

35 Signature:

D. Moses Jeyakaran
Advocate & Patent Agent
IN/PA — 369

CELLULOSE DERIVED GRAPHENIC FIBERS FOR CAPACITIVE DESALINATION
5 OF BRACKISH WATER AND PREPARATION METHOD OF THE ELECTRODE
THEREOF

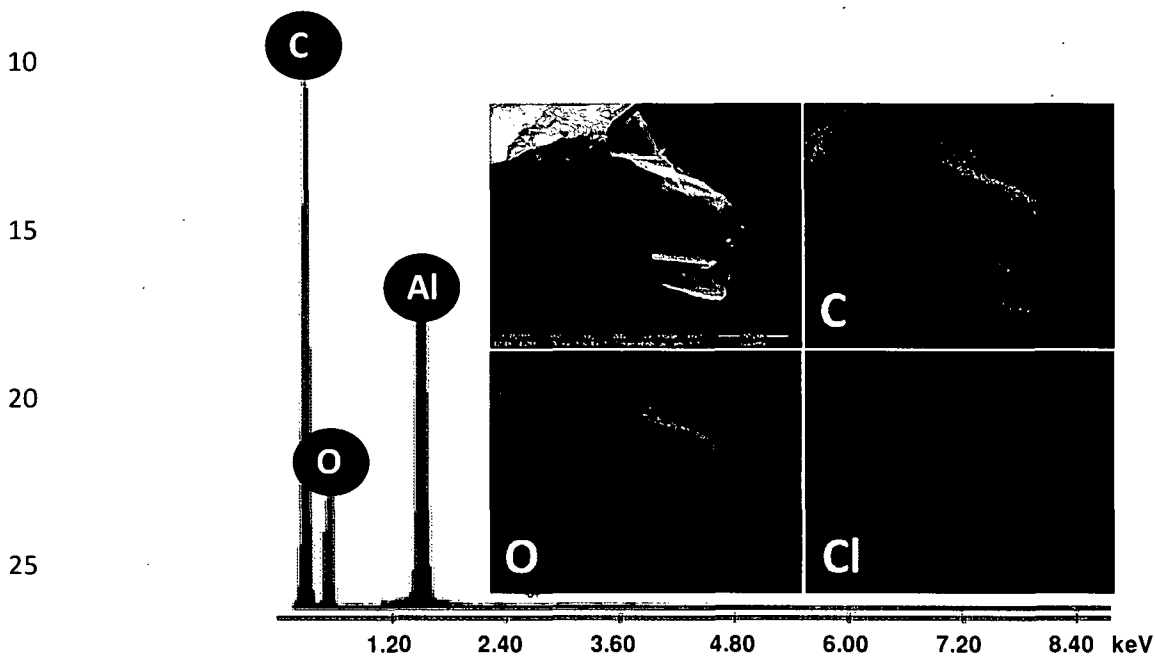


FIGURE 12

Signature:

D. Moses Jeyakaran
Advocate & Patent Agent
IN/PA — 369

5 CELLULOSE DERIVED GRAPHENIC FIBERS FOR CAPACITIVE DESALINATION
OF BRACKISH WATER AND PREPARATION METHOD OF THE ELECTRODE
THEREOF

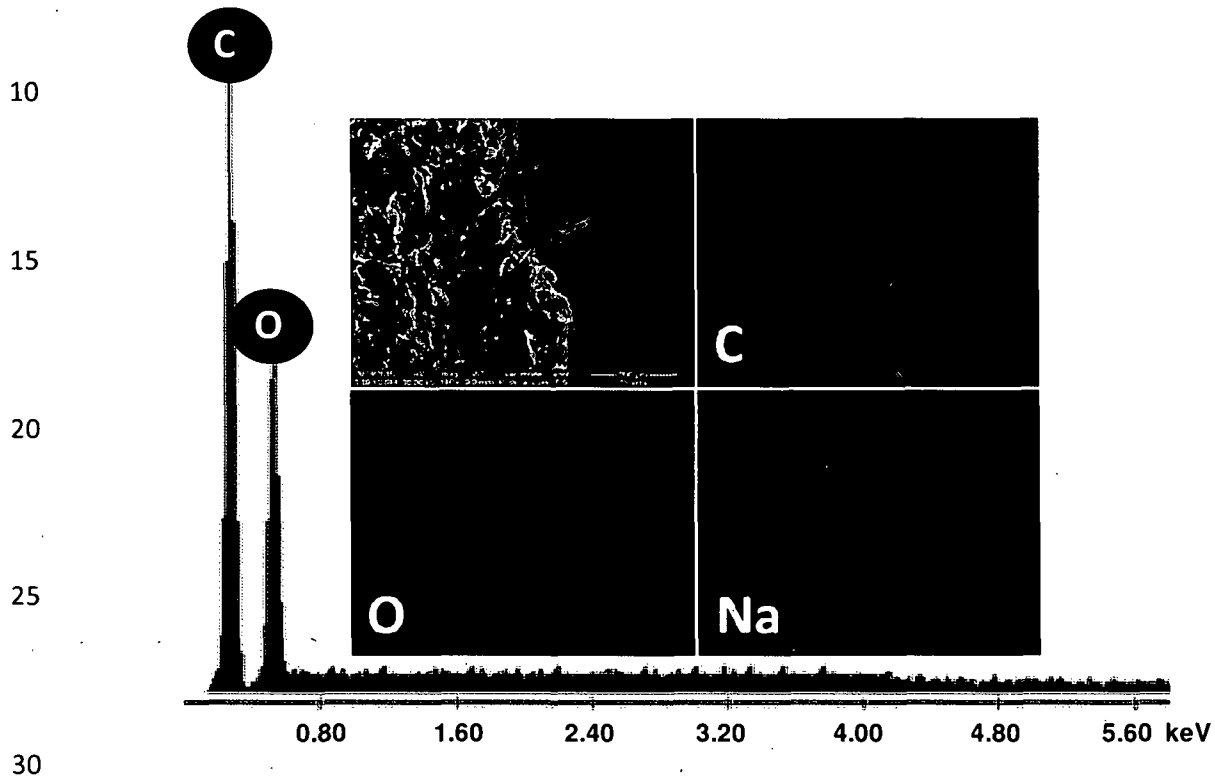


FIGURE 13

Signature:

D. Moses Jeyakaran
Advocate & Patent Agent
IN/PA — 369

5 CELLULOSE DERIVED GRAPHENIC FIBERS FOR CAPACITIVE DESALINATION
 OF BRACKISH WATER AND PREPARATION METHOD OF THE ELECTRODE
 THEREOF

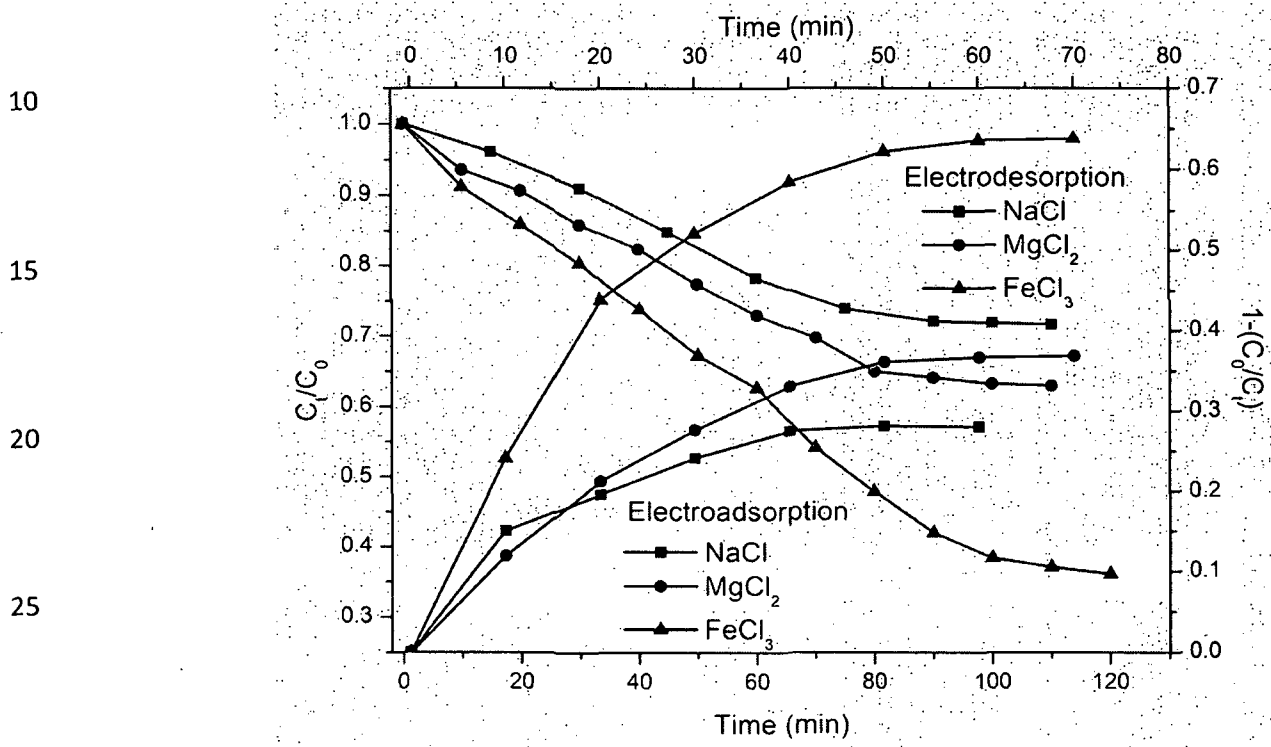


FIGURE 14

Signature: *D. Moses Jeyakaran*

D. Moses Jeyakaran
 Advocate & Patent Agent
 IN/PA — 369

5 CELLULOSE DERIVED GRAPHENIC FIBERS FOR CAPACITIVE DESALINATION OF BRACKISH WATER AND PREPARATION METHOD OF THE ELECTRODE THEREOF

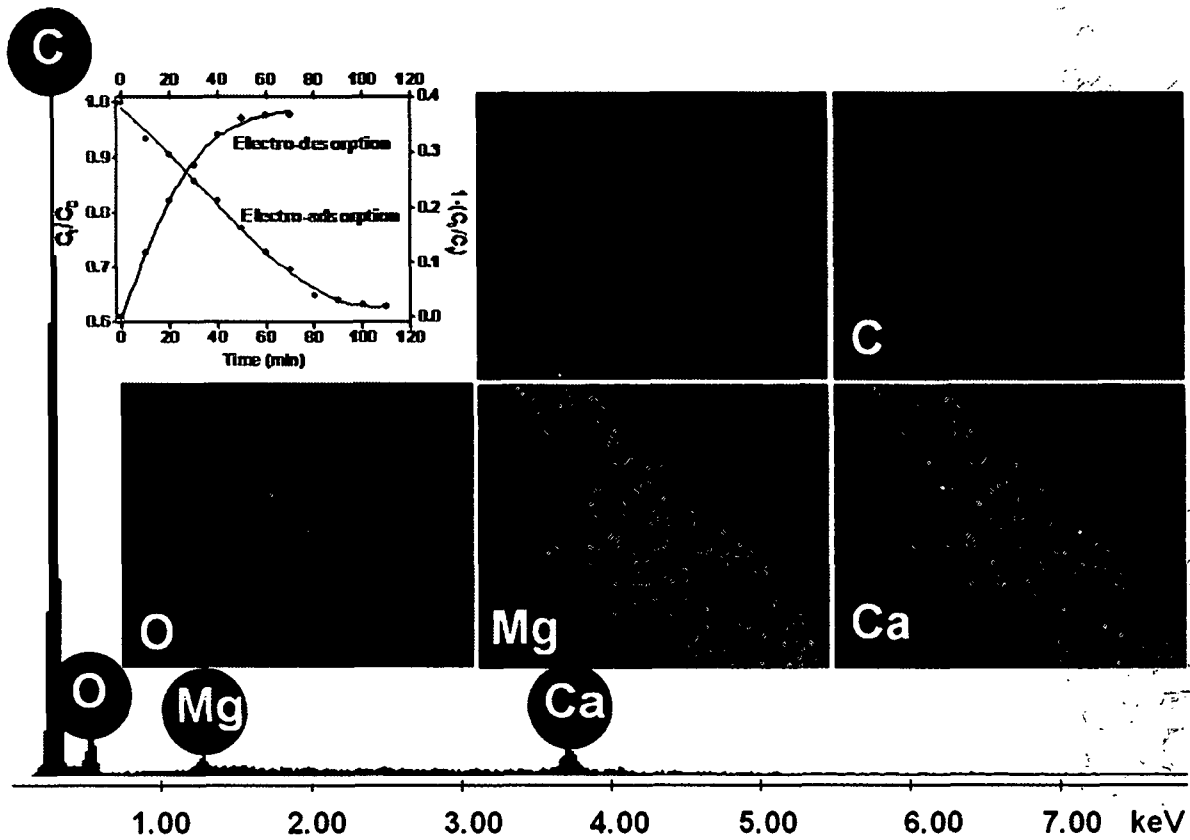


FIGURE 15

Signature: *[Handwritten Signature]*

D. Moses Jeyakaran
Advocate & Patent Agent
IN/PA — 369

5 CELLULOSE DERIVED GRAPHENIC FIBERS FOR CAPACITIVE DESALINATION
OF BRACKISH WATER AND PREPARATION METHOD OF THE ELECTRODE
THEREOF

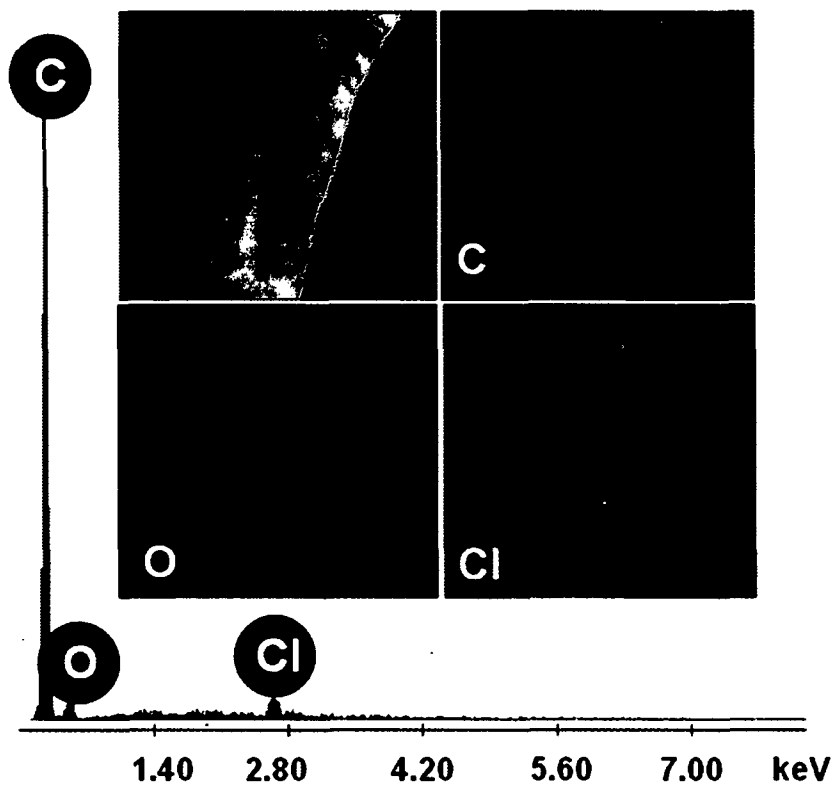


FIGURE 16

Signature: *D. Moses Jeyakaran*

D. Moses Jeyakaran
Advocate & Patent Agent
IN/PA — 369

5 CELLULOSE DERIVED GRAPHENIC FIBERS FOR CAPACITIVE DESALINATION OF BRACKISH WATER AND PREPARATION METHOD OF THE ELECTRODE THEREOF

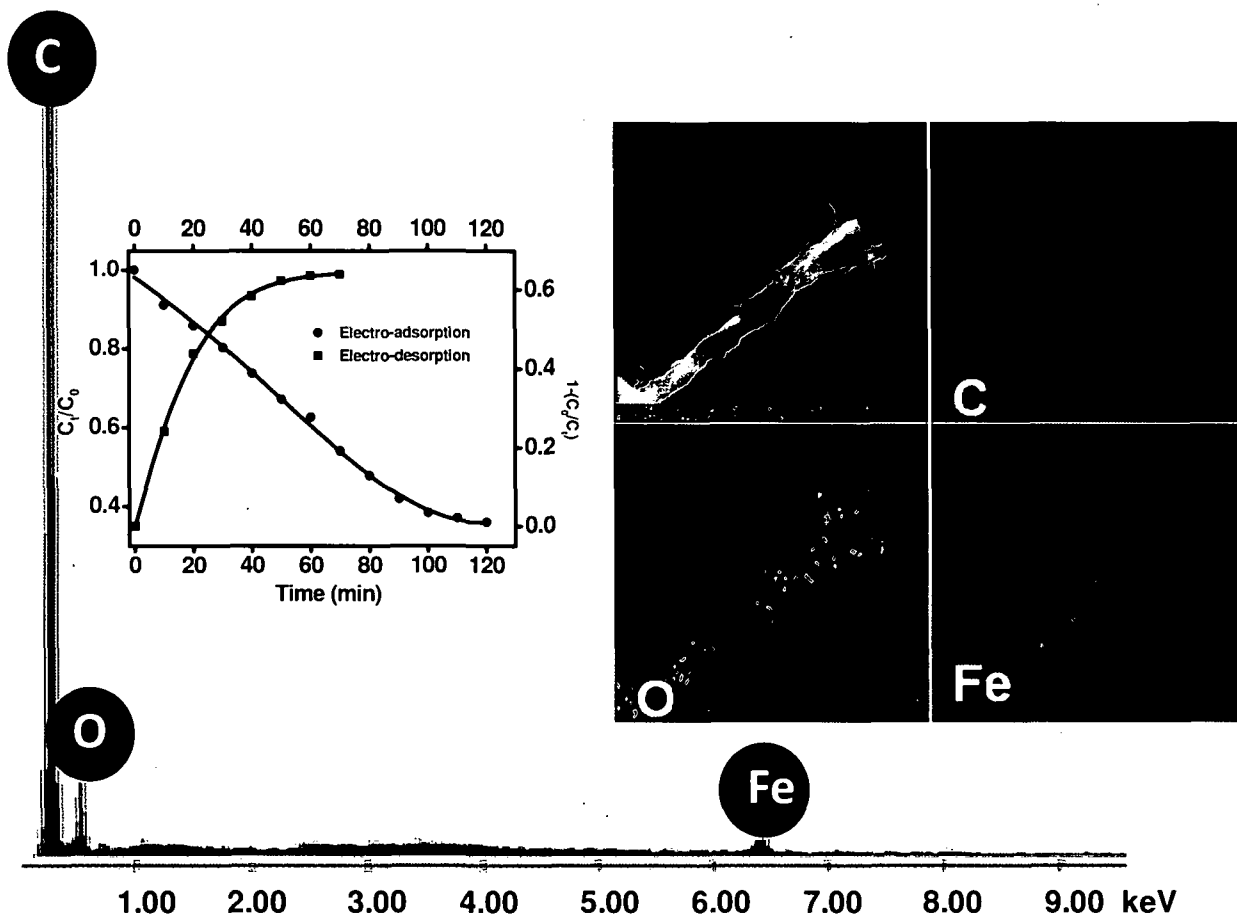


FIGURE 17

Signature: *D. Moses Jeyakaran*

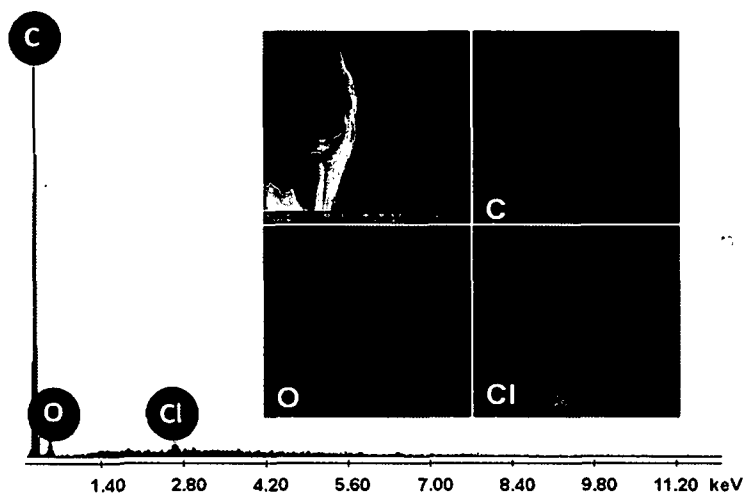
D. Moses Jeyakaran
 Advocate & Patent Agent
 IN/PA — 369

10

15

20

5 CELLULOSE DERIVED GRAPHENIC FIBERS FOR CAPACITIVE DESALINATION
OF BRACKISH WATER AND PREPARATION METHOD OF THE ELECTRODE
THEREOF



10 **FIGURE 18**

15 Signature: *D. Moses Jeyakaran*

20 D. Moses Jeyakaran
Advocate & Patent Agent
IN/PA — 369

5 CELLULOSE DERIVED GRAPHENIC FIBERS FOR CAPACITIVE DESALINATION OF BRACKISH WATER AND PREPARATION METHOD OF THE ELECTRODE THEREOF

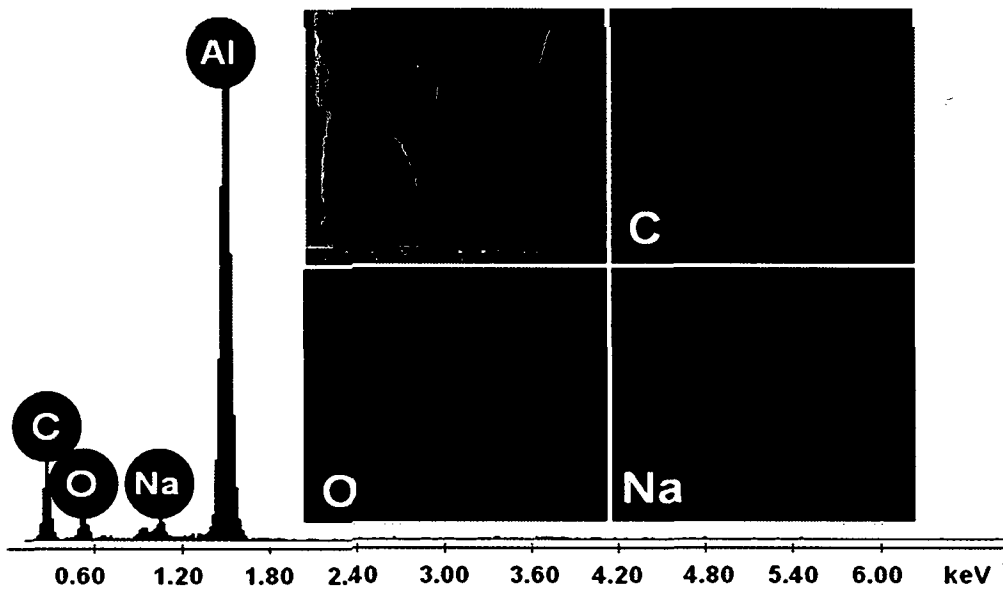


FIGURE 19

Signature: *D. Moses Jeyakaran*

D. Moses Jeyakaran
Advocate & Patent Agent
IN/PA — 369

CELLULOSE DERIVED GRAPHENIC FIBERS FOR CAPACITIVE DESALINATION OF BRACKISH WATER AND PREPARATION METHOD OF THE ELECTRODE THEREOF

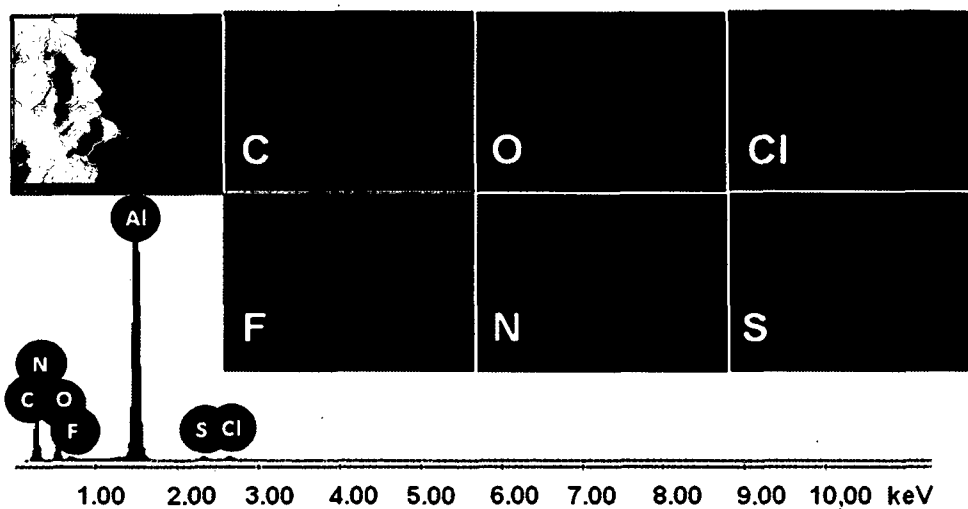


FIGURE 20

Signature: *D. Moses Jeyakaran*

D. Moses Jeyakaran
Advocate & Patent Agent
IN/PA — 369